Proceedings of the IASS 2024 Symposium
Redefining the Art of Structural Design
August 26-30, 2024, Zurich, Switzerland
Philippe Block, Giulia Boller, Catherine DeWolf,
Jacqueline Pauli, Walter Kaufmann (eds.)

Robust funicularity of arches via adaptive shape control

Péter L VÁRKONYI*, Andres F. GUERRA RIAÑO[a]

*,[a] Budapest University of Technology and Economics, Budapest, Hungary
Muegyetem rkp. 3, Budapest, 1111, Hungary
varkonyi.peter@epk.bme.hu

Abstract

Funicular arches balance their loads through axial forces, which makes them more material-efficient than structures subject to bending. Funicularity means that the structure's shape must match its loads, thus funicular arches tend to behave poorly if the distribution of loads varies over time. Flexible cables adapt their shapes passively to varying loads and remain funicular but arches under compression need sufficient bending stiffness, and thus are not capable of passive shape adaptation. In this work we explore the design paradigm of robust funicularity via active shape adaptation. Inspired by slender plant organs, we envision an autonomous structural system, which actively responds to internal bending by developing curvature, until funicularity is restored. In previous work, we investigated a discrete model of a cantilever structure in which rotary actuators driven by standard PID controllers were able to drive the system towards funicular forms using local torque measurements. In the current work, we apply similar ideas to a four-bar linkage mechanism considered to be a discretized model of a funicular arch. We find that if several joints are actuated, the system may be in a state of self-stress due to incompatible settings of the actuators. This unwanted phenomenon makes autonomous operation of the individual actuators challenging. We propose control laws that overcome this difficulty, present dynamic simulation of the structure and its actuators and verify linear stability of the funicular shape analytically.

Keywords: Funicular structures, adaptive structures, shape control, PID controller, stability

1. Introduction

Funicular arches are material efficient structures since they transfer loads only through axial forces. In order to eliminate shear and bending, structural shape must be determined based on the load trajectory, using form-finding methods. [1] [2] (Fig. 1A). In real life, loads are usually time-dependent. In the case of funicular arches subject to compression, variation of the load destroys funicularity (Fig. 1B-C). [3] [4]. In contrast, flexible cable structures autonomously adjust their shapes in response to varying loads while maintaining funicularity [5] (Fig. 1D), which enables extremely lightweight design solutions. Inspired by this performance, and by natural behaviors observed in plants, which adapt actively to changing external conditions [6], we aim to study structures, which remain funicular under time-dependent loads, but operate primarily under compression.

As a promising solution, adaptive structures possess the capability to modify both their physical shape and structural attributes to achieve specific objectives or to meet particular needs. Implementation can occur via remote control or via automated processes responding to external stimuli. This field integrates various disciplines, including materials science, actuation technologies, sensor development, control systems, composite materials, structural engineering, and dynamics [7]. Common applications of adaptive structures are found in the aerospace industry and space exploration. However, these systems have also been utilized in architecture and structural engineering for structural health monitoring [8], vibra-

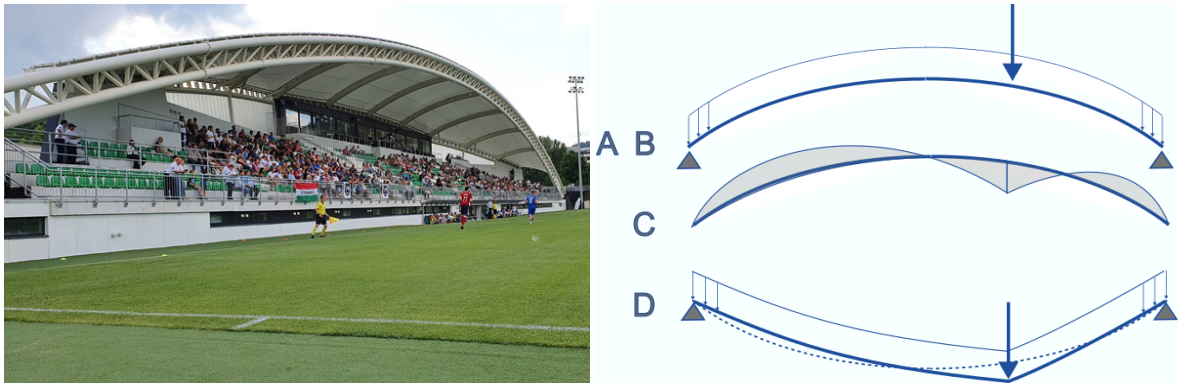

Figure 1: The lightweight, and slender main girder of the BSC Stadium in Budaors, Hungary (A) is a funicular arch for uniform vertical load. An added concentrated load (B) would induce bending in the arch (C), which may lead to failure. In contrast, a cable changes its shape in response to variable load to maintian funicularity (D).

tion control through local feedback [9], shape control of trusses [10], and as active earthquake protection [11].

Here, we investigate a simplified, discrete model of an arch, composed of a chain of straight bars assembled with pin joints and rotary actuators. It is assumed that load variations are *neither predictable, nor directly measurable*, thus direct calculation of the target form is not feasible. Nevertheless the current structural state can be measured. We employ a feedback control strategy, whereby actuators are driven by PID (Proportional-Integral-Derivative) controllers. By appropriately tuning the control parameters to react in proportion to deviations from the desired funicular shape, we manage to maintain functionality using a novel error function.

In Section 2, we introduce the mechanical model of the arch. The equations of motion of the model are determined through a Lagrangian approach similar to our previous work on cantilevers [12, 13]. In Section 3, we undertake an investigation of an unconventional error function incorporated to the control policies. This unique approach enables to develop a form of torque control, which allows to find and keep funicular shapes. Finally, in Section 4, we perform stability analysis. By employing simulations and conducting linear stability analyses, we study the influence of initial conditions, the effects of varying loads, and the impact of control parameters on the system's behavior.

2. Dynamics of a four-bar linkage with actuators

The discrete arch model composed of 3 bars is better known as a planar four-bar linkage (Figure 2A). The model is equipped with pin support at points 0 and 3, hinge connections at 1, 2, and rotary actuators at all 4 points. For simplicity mass is assumed to be concentrated in equal masses $m_i = 1$ located at the hinges (but more realistic mass distributions could easily be implemented). External loads $F_i = (F_{ix}, F_{iy})$ are located at points $i = 1, 2$. In order to avoid the complex kinematics of closed chains, we perform computations on a model in which the rigid support at point 3 is replaced by a linear spring with high elastic constant E_d, which attracts mass m_3 to a preferred position (x_{3p}, y_{3p}) (Figure 2B). The modified model allows us to use the cantilever model [13] with an additional external force.

Equations of motion are derived employing Euler-Lagrange equations using the tangent angles a_0, a_1, a_2 (Fig. 2B), and their derivatives $\dot{a}_i$ with respect to time as state variables. In a reference coordinate frame

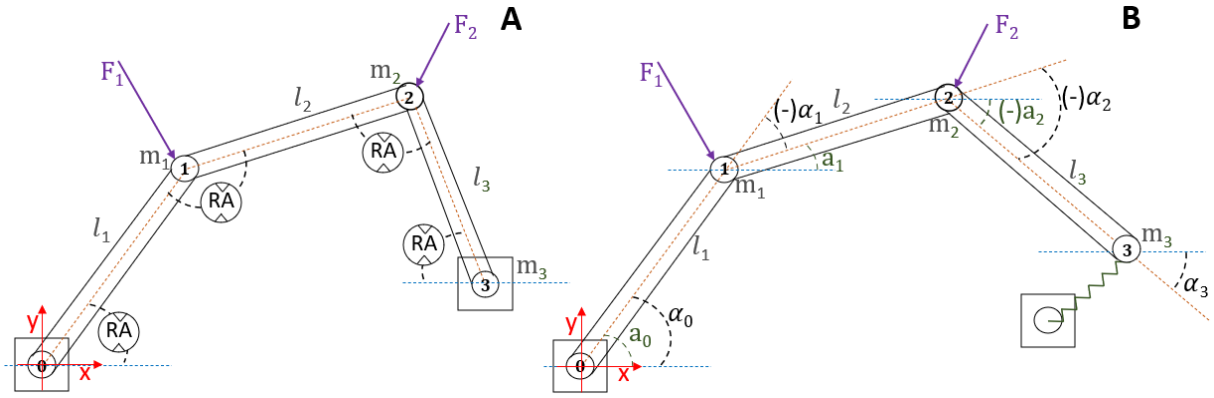

Figure 2: A: Mechanical model of discrete arch equipped with rotary actuators (RA); B: modified cantilever model with compliant support at point 3, and the kinematic variables. Negative angles are marked by $(-)$ sign.

with origin at support 0, position coordinates (r_{ix}, r_{iy}) of mass i can be written as:

$$r_{1x} = l_1 \cos a_0;\ r_{1y} = l_1 \sin a_0 \tag{1}$$

$$r_{2x} = r_{1x} + l_2 \cos a_1;\ r_{2y} = r_{1y} + l_2 \sin a_1 \tag{2}$$

$$r_{3x} = r_{2x} + l_3 \cos a_2;\ r_{3y} = r_{2y} + l_3 \sin a_2 \tag{3}$$

The kinetic energy of the system is:

$$T = \frac{1}{2}\left[m_1(\dot{r}_{1x}^2(t) + \dot{r}_{1y}^2(t)) + m_2(\dot{r}_{2x}(t) + \dot{r}_{2y}^2(t)) + m_3(\dot{r}_{3x}^2(t) + \dot{r}_{3y}^2(t))\right], \tag{4}$$

The potential energy associated to the external forces and the linear spring at point 3 is given by

$$V = -F_{1y}r_{1y} - F_{2y}r_{2y} - F_{1x}r_{1x} - F_{2x}r_{2x} + \frac{1}{2}E_d\left[(r_{3x} - x_{3p})^2 + (r_{3y} - y_{3p})^2\right], \tag{5}$$

and the Lagrangian is calculated as $L = T - V$.

Torques delivered by rotary actuators in the joints will be denoted as τ_i. The generalized force vector (g_0, g_1, g_2) due to actuator action is given by

$$g_i = \frac{\partial \alpha_0}{\partial a_i}\tau_0 + \frac{\partial \alpha_1}{\partial a_i}\tau_1 + \frac{\partial \alpha_2}{\partial a_i}\tau_2 + \frac{\partial \alpha_3}{\partial a_i}\tau_3 \tag{6}$$

where the relative angles of adjacent bars are defined as

$$\alpha_0 = a_0;\ \alpha_1 = a_1 - a_0;\ \alpha_2 = a_2 - a_1; \alpha_3 = -a_0 - a_1 - a_2. \tag{7}$$

By solving Euler-Lagrange equations

$$\frac{\partial}{\partial t}\left(\frac{\partial}{\frac{\partial}{\partial t}a_i}L\right) = \frac{\partial}{\partial a}L + g_i, \tag{8}$$

we obtain for the angular acceleration vector $\gamma = [\ddot{a}_0(t), \ddot{a}_1(t), \ddot{a}_2(t)]^T$ a lengthy closed-form expression, which is omitted for brevity.

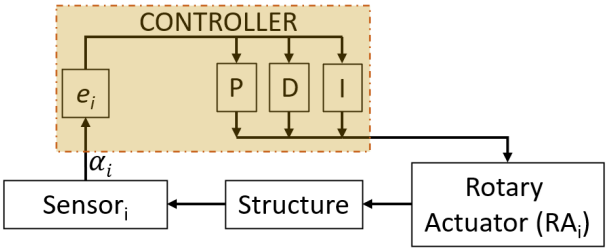

Figure 3: A closed-loop operation of a PID control system with continuous feedback.

3. Funicular shape control of a discrete arch using PID controllers

Our main goal is to design a feedback controller, which is able to choose the actuators' torques τ_i in such a way that the structure converges to and maintains a funicular shape. The main challenge lies in that the loads and thus the target shapes are unknown to the controller. We propose to choose standard PID (Proportional-Integral-Derivative) controllers, common in industrial applications. The action (in this case: torque) of a PID controller is the sum of proportional, derivative, and integral components: $\tau_i(t) = \tau_i^P(t) + \tau_i^D(t) + \tau_i^I(t)$. The individual terms of actuator i depend on an error functions $e_i(t)$ as

$$\tau_i^P(t) = -K_{Pi}\, e \tag{9}$$

$$\tau_i^D(t) = -K_{Di}\dot{e}_i(t) \tag{10}$$

$$\tau_i^I(t) = K_{Ii} \int_0^t e(\theta)\, d\theta. \tag{11}$$

Here, $\tau_i^P\,(t)$ is action proportional to the current error, which promotes convergence to the desired state. $\tau_i^I\,(t)$ takes into account the accumulated past errors, and is responsible in most PID controllers for elimination of residual errors on a longer time scale. $\tau_i^D\,(t)$ responds to the time derivative of the error over time, and provides damping to stabilize the system. The weights of the individual terms are set by the three sets of controller gain parameters K_{Pi}, K_{Ii}, and K_{Di}. The design of a PID controller consists of finding an appropriate error function, which represents deviation from the desired state, as well as appropriate values of control gains, which optimize performance. Figure 3 illustrates the control loop: A sensor continuously measures the current structural state and calculates the error, then drives the actuators using the sum of proportional, integral, and derivative terms.

In the current application, it seems natural to define error functions as the deviations of the (easily measurable) current angles $\alpha_i(t)$ from some preferred values λ_i:

$$e_i = \alpha_i(t) - \lambda_i. \tag{12}$$

If λ_i was a constant, this error function would promote shape evolution towards a prescribed shape. Nevertheless, keeping the structure funicular brings an additional challenge because the target shape depends on the loads, which cannot be measured directly. In consequence, the target funicular position is unknown to the controller, hence further development is needed.

At this point, it is instructive to note a physical interpretation of the action of a PID controller with (12). The proportional $\tau_i^P\,(t)$ and derivative $\tau_i^D\,(t)$ terms are equivalent to a linear torsional spring with torque-free angle λ_i, and a linear damper. Additionally, the sum of the proportional and integral terms

can be rewritten as:

$$\tau_i^{PI}(t) = -K_{Pi}(\alpha_i(t) - \bar{\lambda}_i) \tag{13}$$

$$\bar{\lambda}_i(t) = \lambda_i + \frac{k_{Ii}}{k_{pi}} \int_0^t (\alpha_i(\theta) - \lambda_i) d\theta \tag{14}$$

Differentiation of (14) yields

$$\dot{\bar{\lambda}}_i(t) = \frac{k_{Ii}}{k_{pi}}(\alpha_i(t) - \bar{\lambda}_i). \tag{15}$$

In summary, eq. 15 shows that the three terms are equivalent to a damper and a spring with time dependent torque-free angle $\bar{\lambda}_i$, which is varied by the controller with a rate proportional to the error (12).

In order to achieve funicular shape control, a modified error function is proposed. Funicular shapes are characterized by the property that the structure is in (possibly unstable) static equilibrium in the absence of actuator action. Being static means $\tau_i^D(t) = 0$, hence funicularity requires a sustained equilibrium state with $\tau_i^{PI}(t) = 0$. This condition can be used to find a new funicular error function e_f:

$$e_{fi}(t) = \alpha_i(t) - \bar{\lambda}_i(t) \tag{16}$$

where $\bar{\lambda}_i$ is given by (14), i.e. it is a dynamical quantity, the evolution of which is given by (15).

As a final step, the equations of the system are rewritten in a first order differential equations form, which contains angles a_i, angular velocities ω_i and torque-free angles $\bar{\lambda}_i$ as variables:

$$\dot{y} = f(y), \quad y = (a_0, a_1, a_2, \omega_0, \omega_1, \omega_2, \bar{\lambda}_0, \bar{\lambda}_1, \bar{\lambda}_2, \bar{\lambda}_3)^T \tag{17}$$

where all components of the function f are known in closed form.

As an example, consider an initial condition $y_0 = (\pi/6, 0, -\pi/6, 0, 0, 0, 0, 0, 0, 0)^T$ at time $t = 0$, suppose constant external loads $F_1 = (0, -1)$, $F_2 = (0, -1)$. The preferred position of the second support is $(x_{3p}, y_{3p}) = (2, 0)$, and we assume $E_d = 1000$. The arch is actuated at point 0.

The initial state (dashed blue lines in Figure 3A,C,E) does not respect the preferred position (x_{3p}, y_{3p}) of point 3, hence the structure rapidly jumps into a new configuration in which point 3 is very close to its preferred position (thin purple lines). After this initial transient, point 3 behaves as a pin support. Thereafter, the structure slowly transforms its shape under the action of the controller. Figure 4 shows three examples using different values of gain parameters (Table 1). In two cases, the structure converges to funicular shapes either in pure compression using Parameter set I (Figure 4A), or tension using Parameter set II (Figure 4C). The error functions converge to zero in both cases (Figure 4B,D). The third example uses Parameter set III and fails to converge (Figure 4E). Instead the structure gets stuck at a (non-funicular) configuration subject to a kinematic singularity of the four-bar mechanism, where the torque in the actuator reaches very high values (Figure 4F).

4. Factors affecting convergence to the funicular shape

4.1. Methods of stability analysis

The success of the controller action depends on various factors. A four-linkage mechanism (such as the ideal model of Figure 2A) has 1 degree of freedom, hence, by adjusting the orientation of a single link (as in the previous examples), we can set the shape of the structure. In what follows, we will mostly consider

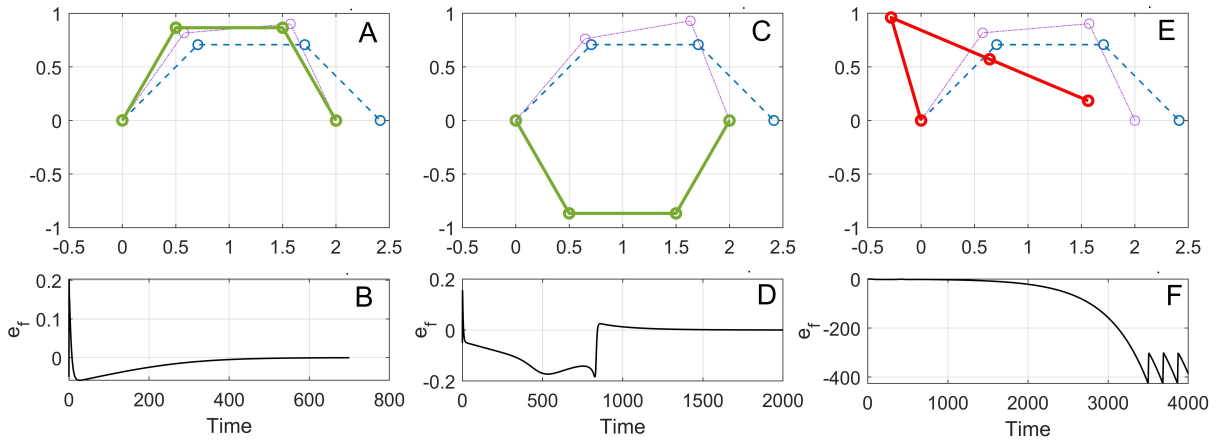

Figure 4: Simulation of shape evolution towards a funicular shape under pure compression using parameter set I (A); towards a shape under pure tension using parameter set II (C); without convergence to a funicular shape using parameter set III (E). Each diagram shows the initial shape at $t = 0$ (dashed line), shape at $t = 24$ after initial fast transient (thin, purple line), and the final shape at the end of the simulation (thick line). The corresponding error functions are depicted in B,D,F.

examples with a single actuator, but the effect of adding multiple actuators will also be discussed briefly.

In previous works we studied a discrete cantilever model [12, 13] with two degrees of freedom, and a unique pure compression funicular shape for any load. The local stability of this shape as a function of controller parameters was successfully investigated using linear stability analysis. We found that an appropriate choice of gain parameters ensures stability for a wide range of load values, furthermore systematical numerical simulations suggested that linear stability indeed implies global stability, i.e. convergence from arbitrary initial state. As we will see, the more complex kinematic and static behavior induced by the second support makes stability margins of an arch more subtle.

We will continue to combine linearization with numerical simulations. In order to assess convergence to a funicular shape in a simulation, we classify a simulation as convergent, if after sufficiently large simulation time, the following bound is satisfied:

$$E_f := |e_{f0}| + |e_{f1}| + |e_{f2}| + |e_{f3}| \leq \Delta. \tag{18}$$

Here, E_f is cumulative error, and Δ is a tolerance value. In our simulations, we used $\Delta = 0.0005$.

In order to carry out linear stability analysis, 17 is linearized at a funicular state y_f as:

$$\dot{y} = f(y) = f(y_f) + J_f(y_f)(y - y_f) + \text{higher order terms} \tag{19}$$

Table 1: Values of controller gains for different simulations to achieve pure compression and tension funicular shapes

Controller gains	Parameter set I	Parameter set II	Parameter set III
K_{P0}	7	7	1
$K_{P1} = K_{P2}$	0	0	0
K_{I0}	-0.002	0.002	-0.002
$K_{I1} = K_{I2}$	0	0	0
K_{Di}	5	5	5

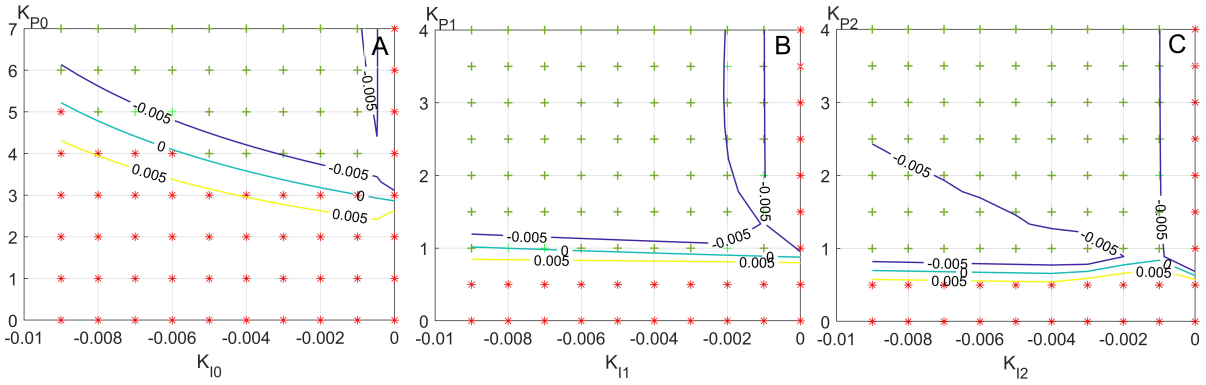

Figure 5: Linear stability analysis, and numerical simulation of shape dynamics for various values of gain parameters using one single actuator at point 0 (A), 1 (B) or 2 (C). Contour lines depict the real part of the leading eigenvalue of the Jacobian (where negative values correspond to stability). Markers show convergent (+) and non-convergent (*) simulations for initial condition specified in the main text.

where $J_f(y_f)$ represents the Jacobian matrix of $f(y)$ and contains the control parameters K_{Pi}, K_{Di} and K_{Ii}. As the funicular shape is in equilibrium, $f(y_f) = 0$ and the high order terms are neglected. The system is linearly stable if the real parts of all eigenvalues of $J_f(y_f)$ are negative. We calculate J_f in closed form using Symbolic Toolbox in MatLab software, and the eigenvalues are evaluated numerically.

4.2. Tuning control parameters

The aim of parameter tuning is to select proper controller gains, which guarantee stability, reduce undesired oscillations, and allow us to achieve funicularity in a convenient time. Here our goal is to illustrate the effect of gains on stability using a parametric study. We consider the same values of (x_{3p}, y_{3p}), E_d, and initial condition as before, along with loads $F_1 = F_2 = (0, -1)$. We assume one actuator at point i (either $i = 0$, $i = 1$, or $i = 2$). The derivative gain is kept constant $K_{Di} = 5$, and different combinations of proportional and integral gains are evaluated through simulations and linear stability analysis. Figure 5A, shows the structural performance when $i = 0$. We see that sufficiently large proportional gain, as well as negative but not too large integral gain are needed to ensure stability. Values inside the stable zone were used in the simulation that appears in Figure 4A. Note that by reducing the value of the proportional gain the system enters the unstable region, which explains lack of convergence in Figure 4E. The cases of $i = 1$ and $i = 2$ (Fig. 5B,C) show similar behavior to one another because of the symmetry of the system (but a small difference is introduced by the assumed elasticity of support 3). In comparison with $i = 0$, smaller value of proportional gain is needed for stability, which indicates that controlling the angle at point 1 or 2 is more advantageous than at point 0.

4.3. The effect of load and initial conditions

The temporal variation of external loads depends on the area of application. If loads change slowly, local stability of the control system is sufficient to maintain funicularity. However, a sudden jump in the external loads may result in a situation where the actual state is far from the desired funicular state. In this case global stability of the system, or the size of the basin of attraction (in the absence of global stability) become crucial questions. Numerical simulations led us to the conclusion that funicular shapes often have relatively large basin of attraction, but they tend to lack global stability. As an illustration, Figure 6A summarizes simulations, in which the load is constant, but different initial conditions $y_0 = (a_0, 0, -a_0, 0, 0, 0, 0, 0, 0, 0)^T$, and integral gains are used. Point 0 is actuated with $k_{P0} = k_{D0} = 5$.

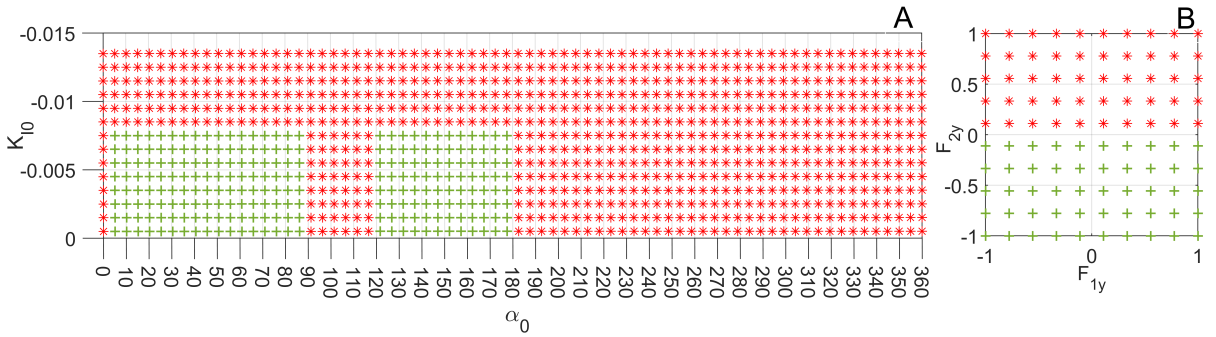

Figure 6: Convergence analysis for different initial geometries and integral gains (A), and an example of the influence of magnitude and direction of load on convergence (B). Markers indicate convergence (+), and non-convergence (*).

We found convergence in two intervals of the initial angle a_0: $(0°, 90°)$ and $(120°, 180°)$. At the same time, convergence occurs only for values of k_{I0} between $(0, -0.08)$, which is explained by the results of linear stability analysis.

Another important practical question is the range of load variations. The magnitude and direction of loads significantly influence the stability, by altering deformation, response dynamics, and internal forces. A reliable controller should ensure stability for all possible values of loads. The influence of load conditions is illustrated by the simulation results of Figure 6B. The vertical loads F_{1y}, and F_{2y} are varied systematically, while initial conditions are $y_0 = (\pi/6, 0, -\pi/6, 0, 0, 0, 0, 0, 0, 0)^T$, and Parameter set I of Table 1 is used. We found convergence for negative values of F_{2y} and for all values of F_{1y}. The asymmetric role of the two loads stems from the asymmetric position of the actuator.

4.4. Actuator interaction

Although setting one single actuator determines the shape of the structure, multiple actuators might have benefits (such as shorter actuation times, or smaller required torques). We make initial steps towards studying the interaction between multiple actuators acting simultaneously. As an example, consider the same load and initial conditions as in the previous section but controlling the arch at point 1 and 2 with $k_{P1} = k_{P2} = 4$, $k_{D1} = k_{D2} = 5$ and $k_{I1} = k_{I2} = -0.005$. Note that each of the two actuators in itself would achieve stability. However, the results depicted in Figure7 show that funicularity is lost with two actuators working simultaneously. Deeper investigation of the results reveals that the two actuators develop increasingly large torques of opposite direction. The diverging support reactions and internal forces eventually drive the system away from the funicular state. This example highlights the possibly detrimental effect of ineraction between actuators if the system is 'overactuated'.

In order get a more detailed picture of interaction, we varied the integral gains, and actuator positions systematically (Figure 8). All simulation results show that stability cannot be achieved unless one of the integral gains is negative, whereas the other is positive and sufficiently large relative to the first one. A useful interpretation of these results can be found if we reconsider the role of the integral term in PID control. An actuator driven by a PID controller with positive integral gain behaves like a torsional spring subject to 'relaxation': over time, the resistance of the spring vanishes. This is 'passive' behavior in the sense, that the work of the actuator is negative. Large and positive integral gain means fast relaxation of the spring, which is similar to a hinge without an actuator. Hence, our numerical results suggest that redundant actuators always tend to generate instability, unless the surplus actuators are ineffective. In other words, the best strategy is to use the minimum number of actuators.

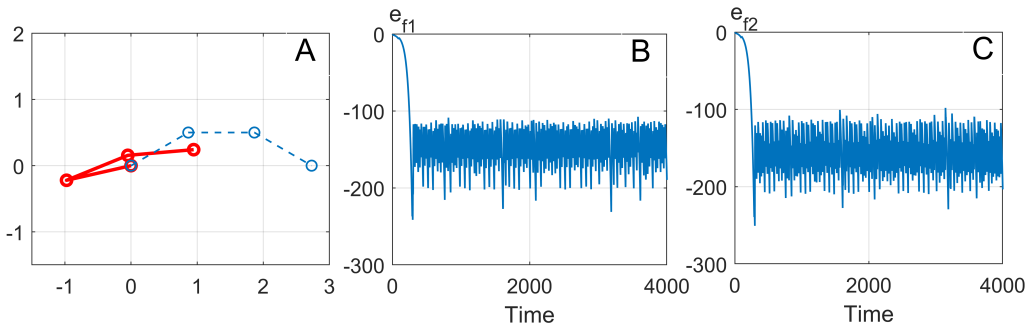

Figure 7: Example of instability produced by the interaction of two actuators. The initial shape (dashed line) does not converge to a funicular configuration (a typical shape is indicated by continuous line) (A), and the error functions for the two actuators (B,C) do not converge to 0.

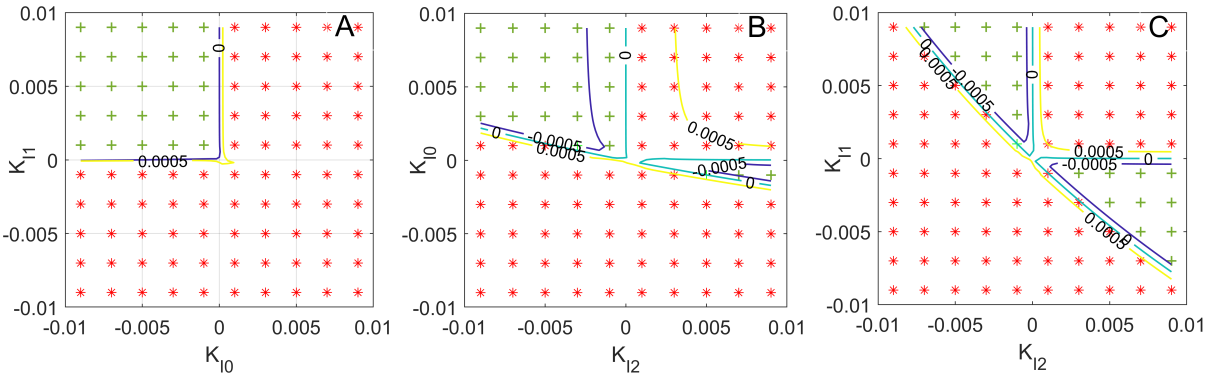

Figure 8: Linear stability analysis and simulations for interaction of two controllers at node 0 and 1 (A), node 0 and 2 (B) and node 1 and 2 (C). In all cases, the two integral gains are varied systematically. The notation is the same as in Fig. 5.

5. Conclusions

We investigated the shape dynamics of a one degree-of-freedom model of an arch under compression. The arch is composed of a 4-bar linkage mechanism equipped with rotary actuators and PID controllers, which can be understood as a toy model of an elastic arch with adjustable intrinsic curvature. First we developed an error function, which is minimized by funicular shapes. Then, a control policy was developed with the intention of robust stabilization of funicular shapes. Importantly, the proposed policy eliminates the need of direct measurements of external loads, or a centralized control unit, as the individual controllers rely on angles of the actuators located at the same joint. The system's stability and robustness were assessed through a combination of linear stability analysis and numerical simulation.

Our investigation shed light to a number of remarkable features. Funicular shapes of pure compression are unstable in the absence of actuators, however the proposed control scheme was able to stabilize them. It was found that the key to stability is sufficiently high proportional and damping terms combined with small and negative integral terms. We also found that the system typically lacks global stability, i.e. initial conditions far from the desired states often do not converge. It was also demonstrated that a controller setup typically provides stability in a range of load values, but stability may be lost outside those regions. These phenomena are crucial for the robustness and reliability of the system, and deserve further investigation. We also investigated redundant actuator setups. It was found, that even if we have two actuators, each of which can stabilize the system individually, they fail to do so if they are applied simultaneously. They drive the system into a state of diverging self-stress, rendering it unstable.

The preliminary results presented in this paper uncover a number of intriguing problems, including the behavior of higher degree-of-freedom models of arches, the robustness of shape control, under varying load, and other performance criteria of shape actuation (such as reaction time). We believe that further exploration of these questions will eventually lead to the birth of a new class of smart and material-efficient structures, which will find its areas of application either in space industry or in architecture.

Acknowledgments

This work has been supported by the National Research, Development and Innovation Fund of the Ministry of Culture and Innovation of Hungary under project K143175.

References

[1] J. Ochsendorf and P. Block, "Exploring shell forms," in *Shell structures for architecture*, Routledge, 2014, pp. 7–14.

[2] M. Bruggi, "A constrained force density method for the funicular analysis and design of arches, domes and vaults," *International journal of Solids and Structures*, vol. 193, pp. 251–269, 2020.

[3] J.-S. Wu and L.-K. Chiang, "Dynamic analysis of an arch due to a moving load," *Journal of Sound and Vibration*, vol. 269, no. 3-5, pp. 511–534, 2004.

[4] P. Clemente, "Introduction to dynamics of stone arches," *Earthquake engineering & structural dynamics*, vol. 27, no. 5, pp. 513–522, 1998.

[5] S. Adriaenssens, P. Block, D. Veenendaal, and C. Williams, *Shell structures for architecture: form finding and optimization*. Routledge, 2014.

[6] M. López, R. Rubio, S. Martín, and B. Croxford, "How plants inspire façades. from plants to architecture: Biomimetic principles for the development of adaptive architectural envelopes," *Renewable and Sustainable Energy Reviews*, vol. 67, pp. 692–703, 2017.

[7] B. K. Wada, "Adaptive structures-an overview," *Journal of spacecraft and rockets*, vol. 27, no. 3, pp. 330–337, 1990.

[8] D. Wagg, I. Bond, P. Weaver, and M. Friswell, *Adaptive structures: engineering applications*. John Wiley & Sons, 2008.

[9] N. Djedoui, A. Ounis, and M. Abdeddaim, "Active vibration control for base-isolated structures using a pid controller against earthquakes," *International Journal of Engineering Research in Africa*, vol. 26, pp. 99–110, 2016.

[10] W. Sobek and P. Teuffel, "Adaptive systems in architecture and structural engineering," in *Smart structures and materials 2001: Smart systems for bridges, structures, and highways*, SPIE, vol. 4330, 2001, pp. 36–45.

[11] R. Guclu, "Sliding mode and pid control of a structural system against earthquake," *Mathematical and Computer Modelling*, vol. 44, no. 1-2, pp. 210–217, 2006.

[12] P. L. Várkonyi and A. F. Guerra Riaño, "From swinging cables to adaptive funicular structures in architecture," in *2022 IEEE 20th Jubilee International Symposium on Intelligent Systems and Informatics (SISY)*, IEEE, 2022, pp. 169–174.

[13] A. F. Guerra Riaño and P. L. Várkonyi, "Shape control of adaptive funicular structures," in *X ECCOMAS Thematic Conference on Smart Structures and Materials SMART 2023*, Eccomas Proceedia, 2023, pp. 679–690.